

Supporting Information

Systematic study of protein labeling by fluorogenic probes using cysteine targeting vinyl sulfone-cyclooctyne tags

Bianka Söveges^[a], Tímea Imre^[b], Tamás Szende^[a], Ádám L. Póti^[c], Gergely B. Cserép^[a],
Tamás Hegedűs^[d], Péter Kele^[a], Krisztina Németh^{[a]*}

[a] B. Söveges, T. Szende, Dr. G.B. Cserép, Dr. P. Kele, Dr. K. Németh

Research Centre for Natural Sciences of Hungarian Academy of Sciences, Institute of Organic Chemistry, Chemical Biology Research Group; H-1117 Budapest, Magyar tudósok krt. 2. Hungary. Tel.: +36 1 382 6659; E-mail address: nemeth.krisztina@ttk.mta.hu

[b] Dr. T. Imre

Research Centre for Natural Sciences of Hungarian Academy of Sciences, Institute of Organic Chemistry, MS Metabolomics Research Group; H-1117 Budapest, Magyar tudósok krt. 2.

[c] Á.L. Póti

Research Centre for Natural Sciences of Hungarian Academy of Sciences, Institute of Enzymology, Protein Research Group; H-1117 Budapest, Magyar tudósok krt. 2. Hungary.

[d] Dr. T. Hegedűs

MTA-SE Molecular Biophysics Research Group, Department of Biophysics and Radiation Biology, Semmelweis University; Tuzolto u. 37-47, H-1094 Budapest, Hungary

Table of Contents

1. Model protein selection based on Cys solvent accessibility	S2
2. Albumin as model protein for labeling with fluorescent linker-dye module	S4
3. Conjugation of p38 with L _{COMBO} and L _{CyO}	S6
4. Testing the stability of fluorogenic dyes on BSA	S7
5. Fluorescent labeling of p38-linker conjugate with fluorogenic dyes	S8
6. Sequential labeling of BSA with linkers and fluorogenic dyes	S9
7. Experimental section	S10
8. References	S20

1. Model protein selection based on Cys solvent accessibility

Several potential candidate proteins of interest carrying thiol group(s) located close to their surface (do not presented in disulfide bonds in their native state) were used for Cys labeling such as serum albumin (human (HSA) or bovine (BSA)), α_1 -acid glycoprotein (AGP), carbonic anhydrase I from human erythrocytes (CA), superoxide dismutase I from bovine erythrocytes (SOD), mitogen-activated protein kinase 14 (p38 α /MAPK14) and extracellular signal-regulated kinase 2 (ERK2).

Although several examples reported on the successful covalent modification of some of these proteins in the presence of detergents and reducing agents,¹⁻³ neither the reductive capacity – studied by Ellman reaction – nor fluorescent conjugation with the vinyl sulfone containing coumarin dye (L_{TAD1}) could be achieved in the absence of detergents even after reducing agent pretreatment in case of (CA, SOD) suggesting that their free cystein residues has low solvent accessibility values. Therefore absolute and relative accessible surface area (ASA, RSA) of their Cys residues were calculated by computational methods (Table S1). In the case of CA and SOD the ASA values of free Cys residues correlate with low tagging probability due to the relatively rigid conformation of proteins. In summary, as expected, the accessibility of the Cys residues can limit the efficiency of the fluorescent derivatization of native proteins.

Since cysteine residues are rarely found on the surface of the proteins; there are two possible ways of labeling: either tagging only the reduced accessible thiol groups while keeping the proteins in their native conformation and function⁴⁻⁶ or pretreatment with detergents and reducing agents (such as dithiothreitol (DTT), mercaptoethanol (ME) or tris(2-carboxyethyl)phosphine (TCEP)) that is required to generate accessible reduced thiols.^{1-3, 7, 8} In our studies, we selected the first approach and made attempts to keep the proteins in their native conformations.

Table S1 Absolute and relative accessible surface area (ASA, RSA) of cysteine residues in proteins

Protein	PDB Code	No. of Cys	ASA (Å ²)	RSA (0.0-1.0)
CA	2CAB	212	0.1	0.001
SOD	1COB	6	2.0	0.014
HSA	1HA2	34	8.7	0.060
AGP	3APU	149*	145.6	0.634
ERK2	1WZY	40	0.0	0.000
		65	0.0	0.000
		127	7.5	0.052
		161	43.4	0.302
		166	1.2	0.008
		216	0.0	0.000
		254	30.3	0.211

CA carbonic anhydrase I (from human erythrocytes)⁹

SOD: superoxide dismutase I (from bovine erythrocytes)¹⁰

HSA: albumin (human serum albumin)¹¹

AGP-A: α_1 -acid glycoprotein A genetic variant¹² (mutant: Cys 149 was replaced by Arg)

ERK2: extracellular signal-regulated kinase 2¹³

2. Albumin as model protein for labeling with fluorescent linker-dye module

Albumin (human and bovine; HSA, BSA)) the most abundant protein and one of the main antioxidants in sera has been chosen as model protein (67 kDa, pI 4.7).^{14, 15} It possesses one – moderately – surface accessible cysteine (Cys 34) (Figure S1A), which is partially reduced (19.8 % and 50.9 % for HSA and BSA, respectively) as it was determined by Ellman reaction (in concordance with data in the literature).^{16, 17} HSA was reacted with six-fold equivalents of the linker-dye conjugate, L_{TA}D₁ (structure: see Figure 2C) under the conditions described previously.¹⁸ Upon addition of L_{TA}D₁ to the protein a surprisingly large fluorescent signal could be detected almost instantaneously as detected by CZE-LIF, which signal further increased within two hours (Figure S1B). The same was observed when the free thiol was inactivated by alkylation with iodoacetamide, indicating that the L_{TA}D₁ binds mainly non-covalently to HSA. This hypothesis was confirmed by affinity chromatography¹⁹ as a $6 \times 10^4 \text{ M}^{-1}$ affinity constant for the L_{TA}D₁ – containing coumarin fluorophor – was evaluated (Figure S1C). We suspect that the well-known warfarin (a 4-hydroxycoumarin derivative) binding pocket (IIA subdomain) of HSA^{11, 20} is responsible for this phenomenon. L_{TA}D₁ affinity towards the warfarin binding pocket was verified by capillary electrophoresis – frontal analysis (CE-FA) method using competitors, warfarin and iodipamide (Figure S1D).

Then, we focused on AGP as other model protein to elaborate their site-selective covalent tagging. This potential candidate failed as well, since it has a ligand binding pocket, too.

These findings draw the attention to the importance of specific/covalent and non-specific/non-covalent interactions since a vast number of proteins have ligand binding capacity and even the commercial fluorescent dyes may contain substructures which can interact with the apolar regions of the proteins (e.g benzotiazoles).²¹⁻²⁴ In addition, one should always keep in mind that several biochemical products contain albumin as stabilizer, which further compromise the selectivity and the signal-to-noise ratio of tagging schemes.

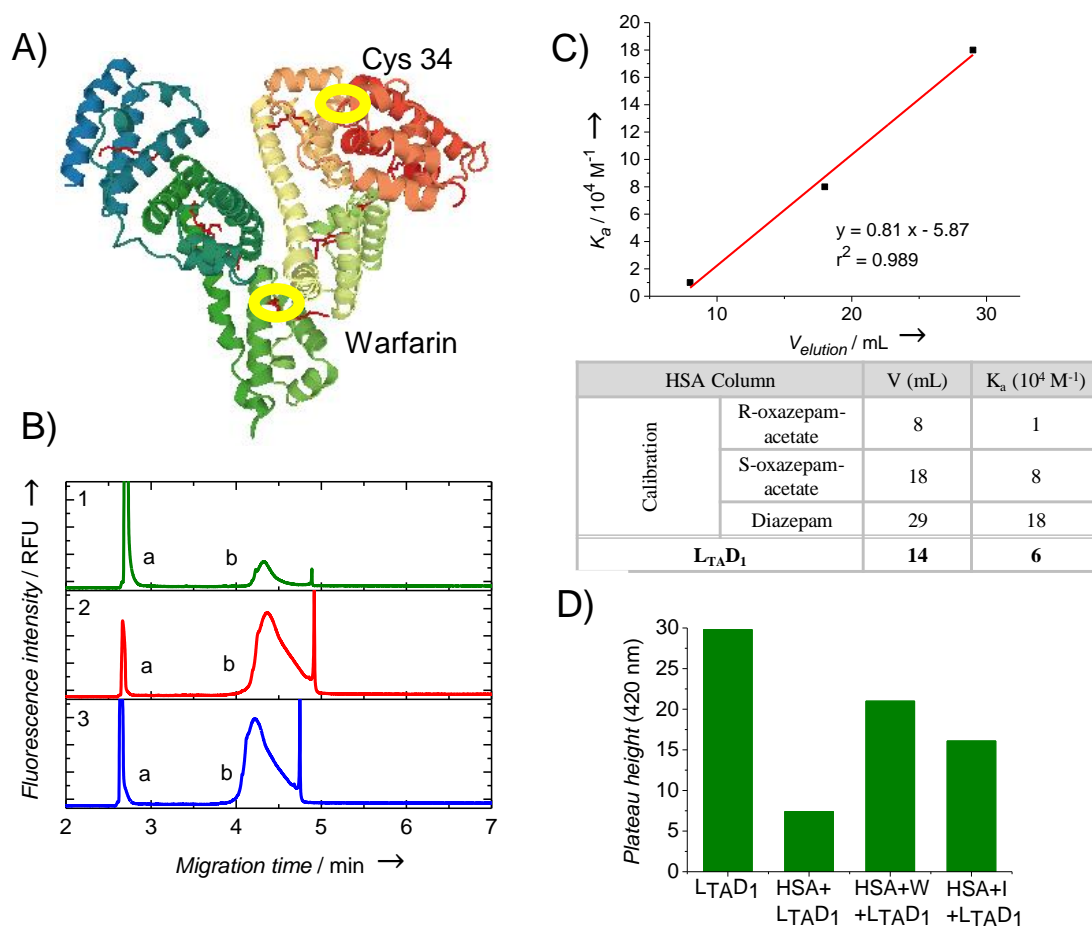


Figure S1.

A: Structure of human serum albumin (Protein Data Bank code 1HA2)¹¹

B: Fluorescent labeling of HSA after 1 minute (1) and 2 hours (2) incubation with L_{TA}D₁ and with alkylation pretreatment (3) monitored by capillary zone electrophoresis with laser induced fluorescent detection.

C: Determination of ligand binding constant of L_{TA}D₁ to HSA by affinity chromatography on HSA-Sepharose column calibrated with ligands of known affinity strength.

D: IIA-site specific ligands (warfarin (W) and iodipamide (I)) partially eliminated association of L_{TA}D₁ (i.e. increased free ligand concentration proportional with plateau height) to HSA as observed by capillary electrophoresis frontal analysis.

3. Conjugation of p38 with L_{COMBO} and L_{CyO}

Efficient conjugation of cyclooctynylated linkers to p38 was proved since subsequent addition of L_{TAD1} did not result in substantial fluorescence signal in SDS-PAGE (Figure S2) compared to the negative control (lane 5). The slight fluorescence signal in lane 5 presumably caused by the reaction between the remaining L_{TAD1} and Cys 39 or 211 which amino acids became accessible during the sample development in SDS due to the unfolding in the presence of the detergent (since Cys 119 and 162 were alkylated upon IAM pretreatment). Mainly this background fluorescence led us to apply native PAGE for further analysis instead of SDS-PAGE.

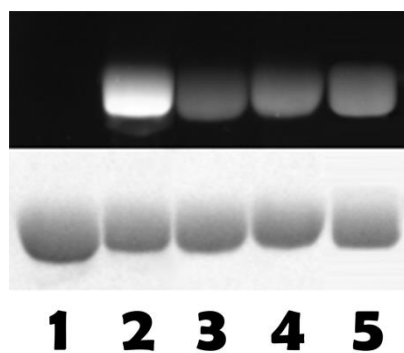
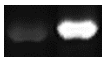
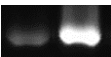
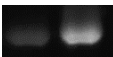
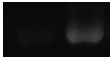
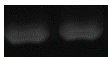
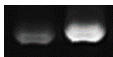


Figure S2. L_{CyO}, L_{COMBO} conjugation saturated the accessible thiols on p38. Samples in SDS-PAGE: Lane 1: p38; Lane 2: p38+L_{TAD1}; lane 3: p38+L_{CyO}+L_{TAD1}; lane 4: p38+L_{COMBO}+L_{TAD1}; Lane 5: p38+IAM pretreatment+L_{TAD1}. Upper picture refers to fluorescent signals ($\lambda_{\text{ex}} = 365 \text{ nm}$), lower picture to Coomassie staining of the gel.

4. Testing the stability of fluorogenic dyes on BSA

Fluorogenic azide dyes D₁-D₆ was added to native and prealkylated BSA. In cases of D₁, D₂, D₃, D₆ an intensive fluorescent band can be seen (in CN-PAGE) in the region of native BSA while there is no substantial fluorescence in the pre-alkylated sample. This suggests that the dyes are reduced by the free Cys 34 of the native BSA and moreover the dyes are associated non-covalently to BSA as one could experience in case of L_{TA}D₁. On the contrary D₄ and D₅ showed no fluorescent signal in the presence of native BSA either (Table S2).

Table S2: Reduction of azide functional group of fluorogenic dyes by reducing agents results in generation of fluorescent signal. In comparison, the evolution of fluorescent signal of dyes (D₁-D₆) incubated with L_{CyO} or L_{COMBO} for two hours is shown.

Dyes		D ₁	D ₂	D ₃	D ₄	D ₅	D ₆
CN-PAGE	BSA + dye						
	alkylation	+ -	+ -	+ -	+ -	+ -	+ -

λ_{ex} : 365 nm for CN-PAGE

5. Fluorescent labeling of p38-linker conjugate with fluorogenic dyes

p38 was successfully, selectively and covalently labeled in consecutive steps by L_{COMBO} and dyes D₁ or D₅ or directly with L_{TA}D₁ (Figure S3).

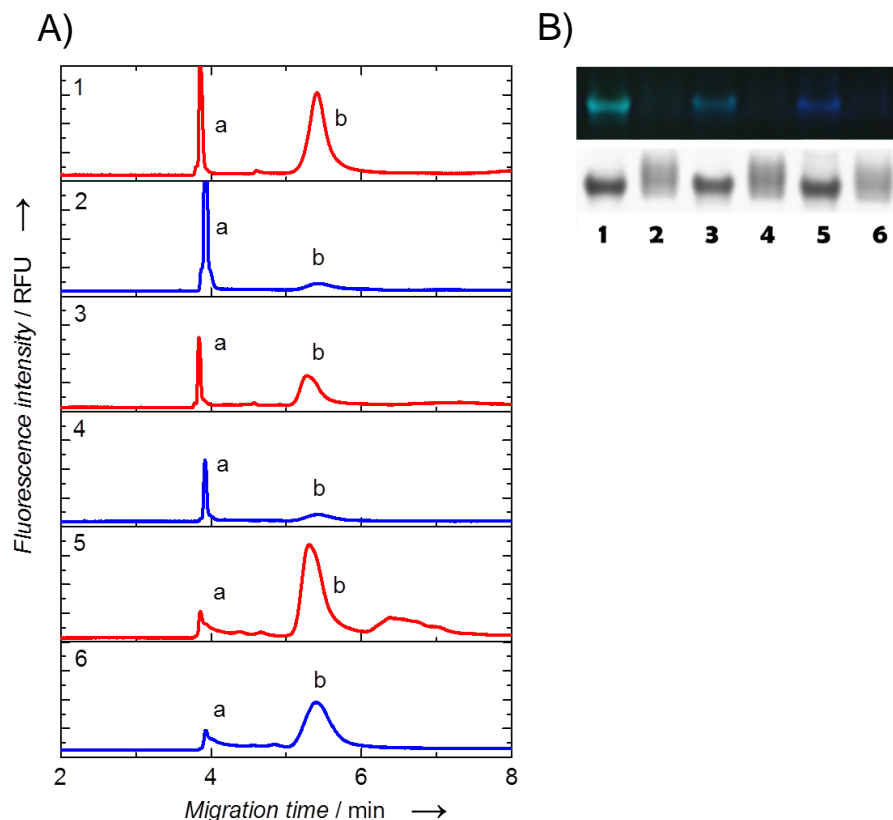


Figure S3. Fluorescent tagging of reduced or prealkylated p38 with L_{TA}D₁ or with L_{COMBO} and dyes D₁ and D₅ monitored by CZE-LIF (A) and CN-PAGE (B). Peak ‘a’: Fluorescent signal of the dye; peak ‘b’: fluorescent signal of the labeled p38. Upper pictures of Figure B refers to fluorescent signals (λ_{ex}= 365 nm), lower pictures to Coomassie staining of the gels.

Samples 1: p38 labeled with L_{TA}D₁; 2: alkylated p38 labeled with L_{TA}D₁; 3: p38 conjugated with L_{COMBO} and labeled with D₁; 4: alkylated p38 conjugated with L_{COMBO} and labeled with D₁; 5: p38 conjugated with L_{COMBO} and labeled with D₅; 6: alkylated p38 conjugated with L_{COMBO} and labeled with D₅.

6. Sequential labeling of BSA with linkers and fluorogenic dyes

We tested BSA in fluorogenic tagging schemes using cyclooctynylated linkers. However, BSA as a model protein has failed again in this context as well. To cut the long story short, regardless that BSA was pre-alkylated or not fluorescent signal was generated upon conjugation of the linker (L_{CyO} , L_{COMBO}) and the dye (D_4 , D_5) (Figure S4), so fluorescent labeling of BSA was also non-specific, non-covalent. This was attributed to BSA's ability to strongly bind the cyclooctynylated linkers too, thus leading to signal evolution upon administration of the fluorogenic dyes. Unfortunately, BSA's affinity towards these linkers was found to be strong enough to prevent appropriate purification.

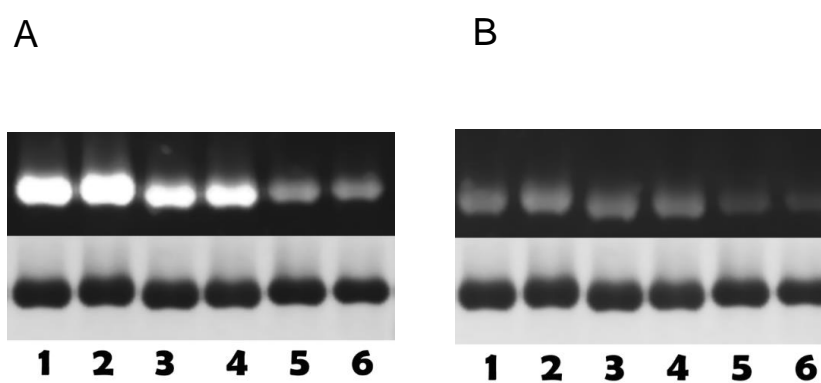


Figure S4. Tagging of BSA – preconjugated with L_{CyO} or L_{COMBO} – with fluorogenic dyes (D_5 (gel A), D_4 (gel B)). Samples on the CN-PAGE gels: Lanes 1: alkylated BSA conjugated with L_{COMBO} and labeled with dye; 2: BSA conjugated with L_{COMBO} and labeled with dye; 3: alkylated BSA conjugated with L_{CyO} and labeled with dye; 4: BSA conjugated with L_{CyO} and labeled with dye; 5: alkylated BSA mixed with dye; 6: BSA mixed with dye. The upper pictures refer to fluorescent signals ($\lambda_{ex}= 365$ nm), lower pictures to Coomassie staining of the gels.

7. Experimental section

Calculation of solvent accessibility of Cys residues in p38

The accessible surface area (ASA) of the proteins were calculated as well by the free online prediction toolkit: <http://cib.cf.ocha.ac.jp/bitool/ASA/> based on the X-ray structures given by the referred PDB Code. This program provides the relative ASA (RSA) value that is the ratio of the surface areas of the corresponding Cys in the protein and in GCG tripeptide (143.79 Å).

Determination of free thiol concentration

250 µL Ellman reagent²⁵ (dithiotreitol, Sigma, (St. Louis, MO, USA)) (400 µM) in 100 mM sodium phosphate buffer (pH 8.0) complemented by 1 mM EDTA (Sigma, St. Louis, MO, USA) was added to 50 µL sample. After 15 min incubation at room temperature in dark the absorbance was determined at 412 nm in quartz cuvette with 1 mm light pathlength by Jasco 7800 UV-Vis spectrophotometer. Freshly prepared cysteine solutions in the 0-1.5 M concentration range were used for calibration.

Affinity chromatography

The elution volume of L_{TAD1} was measured on bromo-cyanide activated and HSA conjugated Sepharose matrix column (Pharmacia Fine Chemicals, Sweden) (4 cm×1 cm) and corrected with the exclusion volume presented on albumin lacking column¹⁹. The strength of ligand binding was evaluated from the calibration curve obtained from drugs (diazepam, and *R*- and *S*-oxazepam-acetate) of known affinity constants²⁶. 10 µL of the 0.5 mg/mL stock solution was injected. Ringer buffer was applied as eluent. Flow rate was 0.85 mL/min.

Capillary electrophoresis frontal analysis

Capillary electrophoresis frontal analysis (CE-FA)²⁷ was performed with an Agilent Capillary Electrophoresis ^{3D}CE system (Agilent Technologies, Waldbronn, Germany) applying bare fused silica capillary having a 64.5 cm total and 56 cm effective length with 50 µm I.D. and bubble cell detector window (Agilent Technologies, Santa Clara, CA, USA). On-line absorption at 420 nm was monitored by DAD UV-Vis detector. The capillary was

thermostated at 25°C. Between measurements, the capillary was rinsed subsequently with 0.1 M HCl, 1.0 M NaOH, 0.1 M NaOH and distilled water for 3 minutes each and with BGE (67 mM phosphate buffer and the pH was adjusted to 7.4 by sodium hydroxide) for 5 minutes. Samples were injected by 5×10^3 Pa pressure for 45 sec. Runs were performed in the positive-polarity mode with 22 kV. The free ligand concentration (proportional with plateau height) of 100 μ M L_{TA}D₁ was determined in the presence and in the absence of human serum albumin and with HSA pretreated with warfarin (100 μ M) or iodipamide (100 μ M).

SDS polyacrylamide electrophoresis experiments

Samples were diluted with sample buffer (62.5 mM Tris-HCl (pH 6.8) + 25 % glycerol + 0.01 % bromophenolblue + 1 % SDS) in 3:1 ratio. The size of the SDS-polyacrylamide gels were 8.5 cm×7.5 cm×0.1 cm. They were the combination of 4 % concentration and 10 % separation PAGE gels (acrylamide:bisacrylamide ratio was 37.5:1; and gel buffers were 500 mM Tris-HCl + 0.4 % SDS (pH 6.8) and 1500 mM Tris-HCl + 0.4 % SDS (pH 8.8), respectively). 7.5 μ g of protein was loaded per lane. Runnings were carried out in Mini-Protean Tetra Cell (Bio-Rad, Hercules, CA, USA) using 25 mM Tris/192 mM glycine; (pH 8.3) + 0.1 % SDS as running buffer and 180 V voltage for 55 min. Furthermore, gels were stained for proteins with Coomassie-Brilliant-Blue.

UV-Vis spectroscopy

Concentration dependency of absorbances at the characteristic maxima of the native protein at 280 nm and that of the L_{TA}D₁ conjugate at 420 nm and 280 nm were determined as well ($\epsilon_{280}^{\text{protein}} = 46000 \text{ M}^{-1}\text{cm}^{-1}$; $\epsilon_{420}^{\text{dye}} = 25000 \text{ M}^{-1}\text{cm}^{-1}$; $\epsilon_{280}^{\text{dye}} = 6800 \text{ M}^{-1}\text{cm}^{-1}$). The protein labeled with L_{TA}D₁ was purified with G25 Sephadex column. Twofold dilution was prepared from all samples. The absorbances at 280 and 420 nm of these samples (n=5) were measured. The concentration of the dye was estimated from the calibration curve. The final protein concentrations of the samples were calculated from the absorbance at 280 nm which were corrected by the contribution of the amount of the dye at this wavelength (Eq. 1). The dye/protein molar ratio was estimated based on the Equation 2 using the absorbances at 280 and 420 nm.^{28,29}

$$[protein\ concentration] = \frac{A_{280}^{protein} - A_{280}^{dye}}{\epsilon_{280}^{protein} \cdot light\ pathlength} \cdot dilution\ factor \quad \text{Eq. 1}$$

$$dye/ protein\ molar\ ratio = \frac{A_{420}^{labelled\ protein}}{\epsilon_{420}^{dye} \cdot [protein\ concentration] \cdot light\ pathlength} \cdot dilution\ factor \quad \text{Eq.2}$$

These estimations however do not take the possible changes of ϵ_{420}^{dye} upon conjugation of the protein into account, here the dye positioned on the surface cysteines and presumably do not associates to the inside regions of the protein therefore no relevant changes in spectral characteristics of the dye is predicted.

Organic syntheses of L_{COMBO} and L_{CyO}

tert-butyl (2-hydroxyethyl)(methyl)carbamate (2)

In a round-bottomed flask flushed with N₂, 1.60 mL 2-(methylamino)-ethanol (19.9 mmol, 1.0 eq.) was dissolved in dry DCM (70 mL), then 4.35 g di-*tert*-butyl dicarbonate (19.9 mmol, 1.0 eq.) in dry DCM (30 mL) was added dropwise. Then the reaction mixture was stirred at room temperature for 14 hours. After completion of the reaction, saturated NH₄Cl (35 mL) was added, then the organic layer was separated. The resulting aqueous layer was extracted with DCM (2 × 100 mL). The combined organic phases were dried over MgSO₄, filtered and evaporated. The crude product was purified by column chromatography (Hex/EtOAc = 1/1 V/V) to give 2.38 g colorless oil (68 %).

R_f = 0.28 (Hex/EtOAc = 2/1 V/V). IR: $\nu(\text{neat}) = 3426, 2975, 2932, 1667, 1392, 1148\text{ cm}^{-1}$. ¹H-NMR (500 MHz, CDCl₃): $\delta = 3.64\text{ (2H, s); } 3.29\text{ (2H, s); } 3.15\text{ (1H, brs); } 2.84\text{ (3H, s); } 1.38\text{ (9H, s)}$. ¹³C-NMR (125 MHz, CDCl₃): $\delta = 155.8; 79.8; 61.1; 51.4; 35.5; 28.4$. HRMS (ESI): calcd for C₈H₁₇NNaO₃⁺ [M+Na]⁺ 198.1101; found 198.1097 (Figure S5).

tert-butyl methyl{2-[2-(vinylsulfonyl)ethoxy]ethyl}carbamate (3)

500 mg (2.85 mmol, 1.0 eq.) **2** and 860 μL (8.55 mmol, 3.0 eq.) DVS were dissolved in 100 mL dry THF in a round-bottomed flask flushed with N₂. To the resulting solution the suspension of 52 mg (0.43 mmol, 0.15 eq.) ^tBuOK and 10 mL abs. THF was added dropwise. After 45 min stirring (following the consumption of the alcohol according to TLC with

Hex/EtOAc=1/1 V/V eluent) the solvent was evaporated. Then the crude product was extracted with 5×15 mL EtOAc, concentrated onto Celite and purified by column chromatography (Hex/EtOAc = 1/1 \rightarrow 1/2 V/V) to give 432 mg (52 %) colorless oil.

$R_f = 0.35$ (Hex/EtOAc = 1/1 V/V). IR: $\nu(\text{neat}) = 2973, 2930, 2490, 1686, 1313, 1156, 1117 \text{ cm}^{-1}$. $^1\text{H-NMR}$ (500 MHz, CDCl_3): $\delta = 6.68$ (1H, m); 6.37 (1H, d, $J = 16.7$ Hz); 6.06 (1H, d, $J = 9.9$ Hz); 3.83 (2H, t, $J = 5.7$ Hz); 3.54 (2H, s); 3.36 (2H, s); 3.21 (2H, t, $J = 5.7$ Hz); 2.86 (3H, s); 1.43 (9H, s). $^{13}\text{C-NMR}$ (125 MHz, CDCl_3): $\delta = 155.8; 137.9; 128.9; 79.7; 66.3; 64.6; 55.1; 53.1; 35.4; 28.5$. HRMS (ESI): calcd for $\text{C}_{12}\text{H}_{23}\text{NNaO}_5\text{S}^+$ $[\text{M}+\text{Na}]^+$ 316.1189; found 316.1180 (Figure S6).

N-methyl-2-[2-(vinylsulfonyl)ethoxy]ethan-1-amine HCl salt (4)

To 20 mL dry methanol 2.4 mL acetyl chloride was added dropwise under N_2 atmosphere at 0°C to give 5 M methanolic HCl solution. Then the solution of 570 mg (1.94 mmol) **3** in dry methanol (5 mL) was added at 0°C and stirred for 4 hours at room temperature. After evaporation of the volatile compounds the desired product was obtained as 436 mg (98 %) yellow oil.

IR: $\nu(\text{neat}) = 2924, 2490, 1673, 1295, 1175, 1116 \text{ cm}^{-1}$. $^1\text{H-NMR}$ (500 MHz, CDCl_3): $\delta = 9.22$ (2H, brs); 6.87 (1H, dd, $J = 16.3$ Hz, 9.3 Hz); 6.39 (1H, d, $J = 16.3$ Hz); 6.16 (1H, d, $J = 9.3$ Hz); 3.93 (2H, s); 3.87 (2H, s); 3.41 (2H, s); 3.17 (2H, s); 2.73 (3H, s). $^{13}\text{C-NMR}$ (125 MHz, CDCl_3): $\delta = 137.3; 130.1; 65.9; 64.3; 54.3; 48.6; 33.7$. HRMS (ESI): calcd for $\text{C}_7\text{H}_{16}\text{NO}_3\text{S}^+$ $[\text{M}+\text{H}]^+$ 194.0845; found 194.0849 (Figure S7).

L_{COMBO}

To the solution of 24.0 mg **5** (0.12 mmol, 1.0 eq.), 42.8 mg HBTU (0.13 mmol, 0.94 eq.) and 18.4 mg HOBT×H₂O (0.12 mmol, 1.0 eq.) in anhydrous DMF (2 mL), 63 µL EDIPA (0.36 mmol, 3.0 eq.) and 30.3 mg **4** (0.13 mmol, 1.1 eq.) were added and stirred for 3 h at room temperature under N₂ atmosphere. After evaporation of the solvent, the remaining residue was purified by column chromatography (DCM/MeOH = 30/1 V/V) to give 9 mg (20 %) product as a colorless oil.

R_f = 0.62 (MeOH/EtOAc = 1/9 V/V). ¹H-NMR (500 MHz, CDCl₃): δ = 7.26-7.21 (2H, m); 7.18 (1H, d, J = 8.2 Hz); 6.79-6.54 (1H, m); 6.40 (1H, d, J = 16.6 Hz); 6.07 (1H, d, J = 9.9 Hz); 3.90 (2H, s); 3.74 (2H, s); 3.55 (2H, s); 3.42 (2H, t, J = 12.6 Hz); 3.25 (2H, s); 3.07 (3H, s); 2.85 (2H, d, J = 12.5 Hz); 2.45 (2H, d, J = 16.1 Hz); 2.28 (2H, t, J = 14.2 Hz). ¹³C-NMR (150 MHz, CDCl₃): δ = 173.6; 143.1; 141.7; 137.8; 134.6; 131.0; 129.7; 129.3; 125.4; 99.4; 99.3; 69.1; 64.7; 55.1; 47.4; 39.0; 37.7; 37.6; 22.8; 22.8. HRMS (ESI): calcd for C₂₀H₂₅NNaO₄S⁺ [M+Na]⁺ 398.1402; found 398.1400 (Figure S8).

L_{CyO}

To the solution of 24 mg **6** (0.10 mmol, 1.0 eq.), 35.6 mg HBTU (0.13 mmol, 0.94 eq.) and 15.3 mg HOBT×H₂O (0.12 mmol, 1.0 eq.) in anhydrous DMF (3 mL), 52 µL EDIPA (0.30 mmol, 3.0 eq.) and 25.3 mg **4** (0.11 mmol, 1.1 eq.) were added and stirred for 3 h at room temperature under N₂ atmosphere. After evaporation of the solvent, the remaining residue was purified by column chromatography (DCM/MeOH = 30/1 V/V) to give 20 mg (47 %) product as a colorless oil.

R_f = 0.64 (MeOH/EtOAc = 1/9 V/V). ¹H-NMR (500 MHz, CDCl₃): δ = 7.26 (2H, d, J = 7.8 Hz); 7.18 (2H, d, J = 7.8 Hz); 6.75-6.45 (1H, m); 6.31 (1H, d, J = 16.6 Hz); 6.00 (1H, d, J = 9.9 Hz); 3.88-3.37 (6H, m); 3.18 (2H, s); 2.98 (3H, s); 2.72-2.51 (3H, m); 2.08 (2H, m); 2.02-1.84 (2H, m); 1.83-1.65 (3H, m); 1.56 (1H, m); 1.37 (2H, m). ¹³C-NMR (125 MHz, CDCl₃): δ = 171.7; 141.9; 137.6; 134.0; 129.0; 128.8; 127.0; 96.4; 94.7; 68.8; 64.5; 54.9; 47.2; 41.6; 40.1; 38.8; 36.5; 34.8; 29.9; 28.4; 20.8. HRMS (ESI): calcd for C₂₃H₃₁NNaO₄S⁺ [M+Na]⁺ 440.1872; found 440.1873 (Figure S9).

Characterization of cyclooctynylated linkers (L_{COMBO}, L_{CyO})

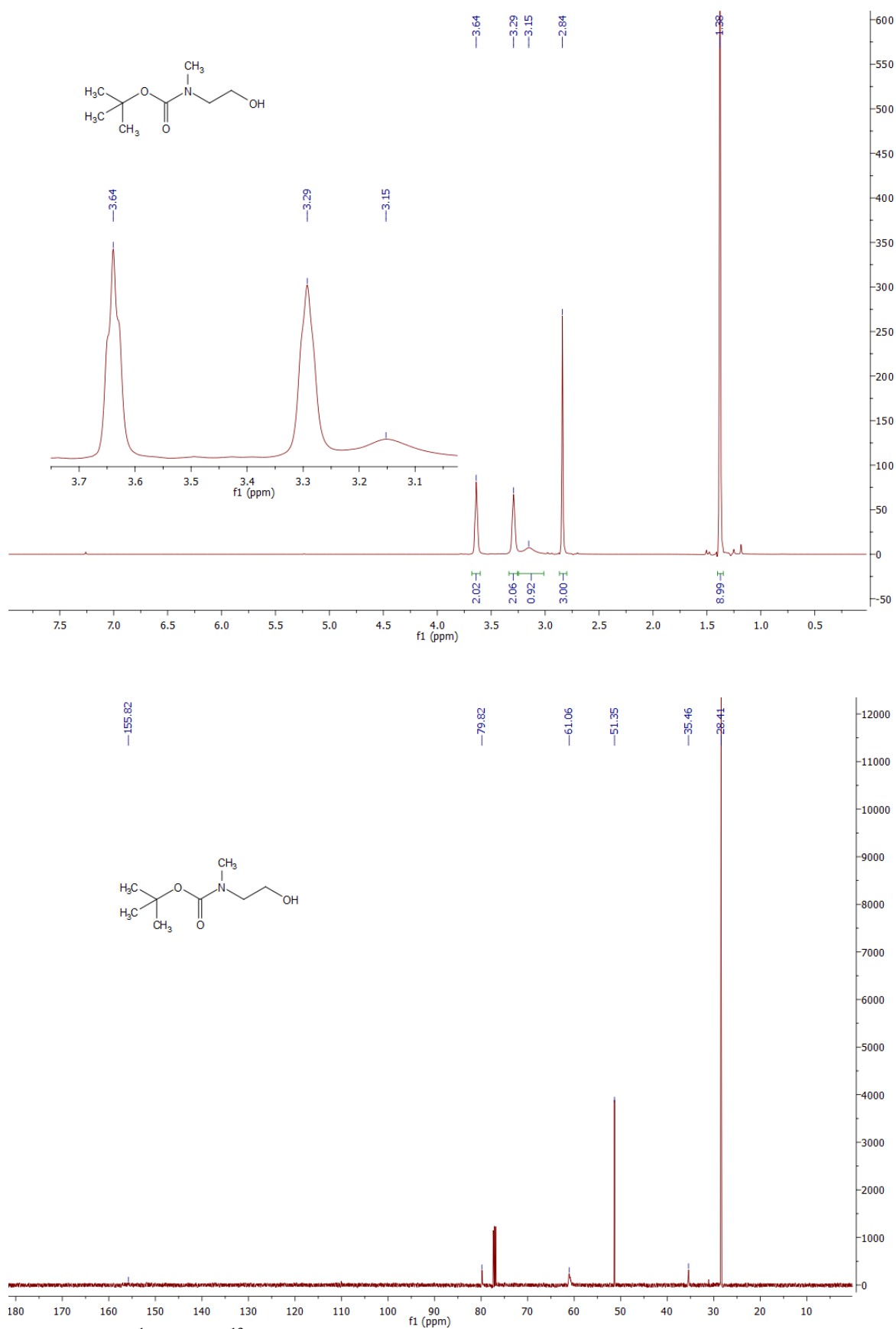


Figure S5. ¹H and ¹³C NMR spectra of *tert*-butyl (2-hydroxyethyl)(methyl)carbamate (**2**)

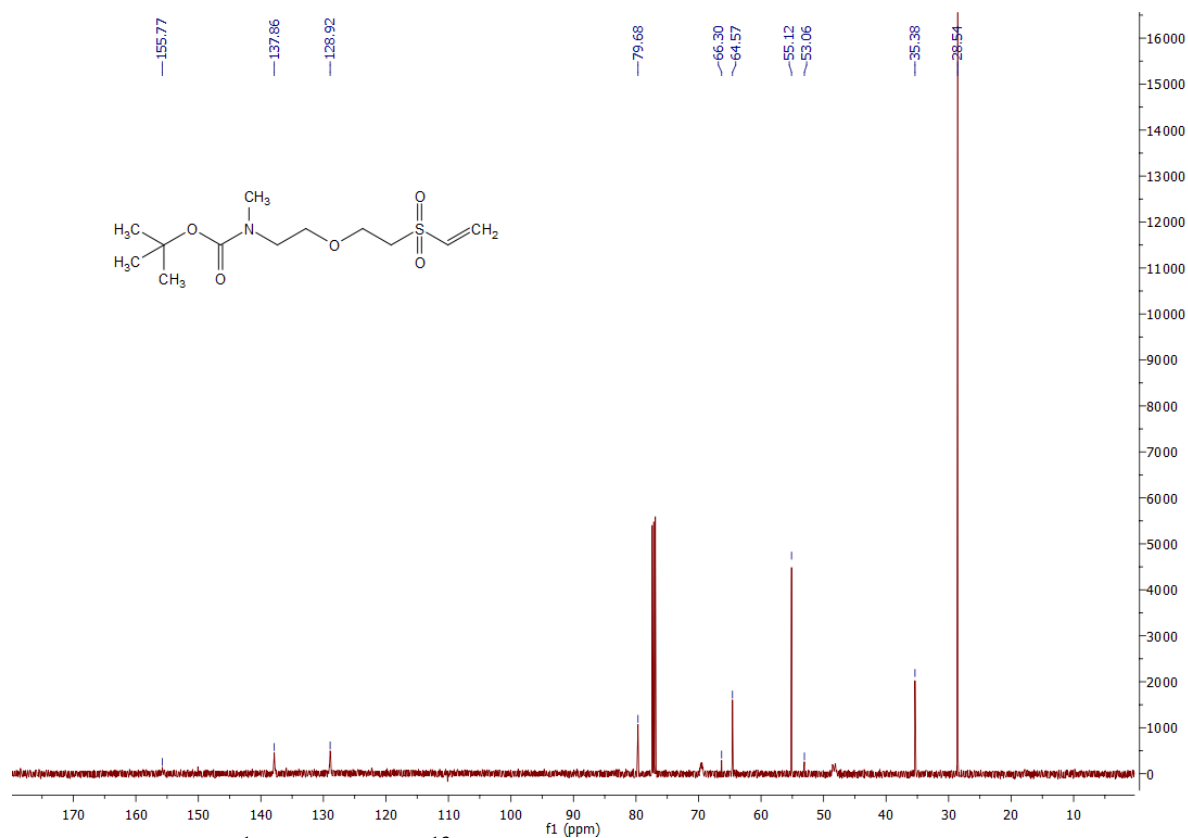
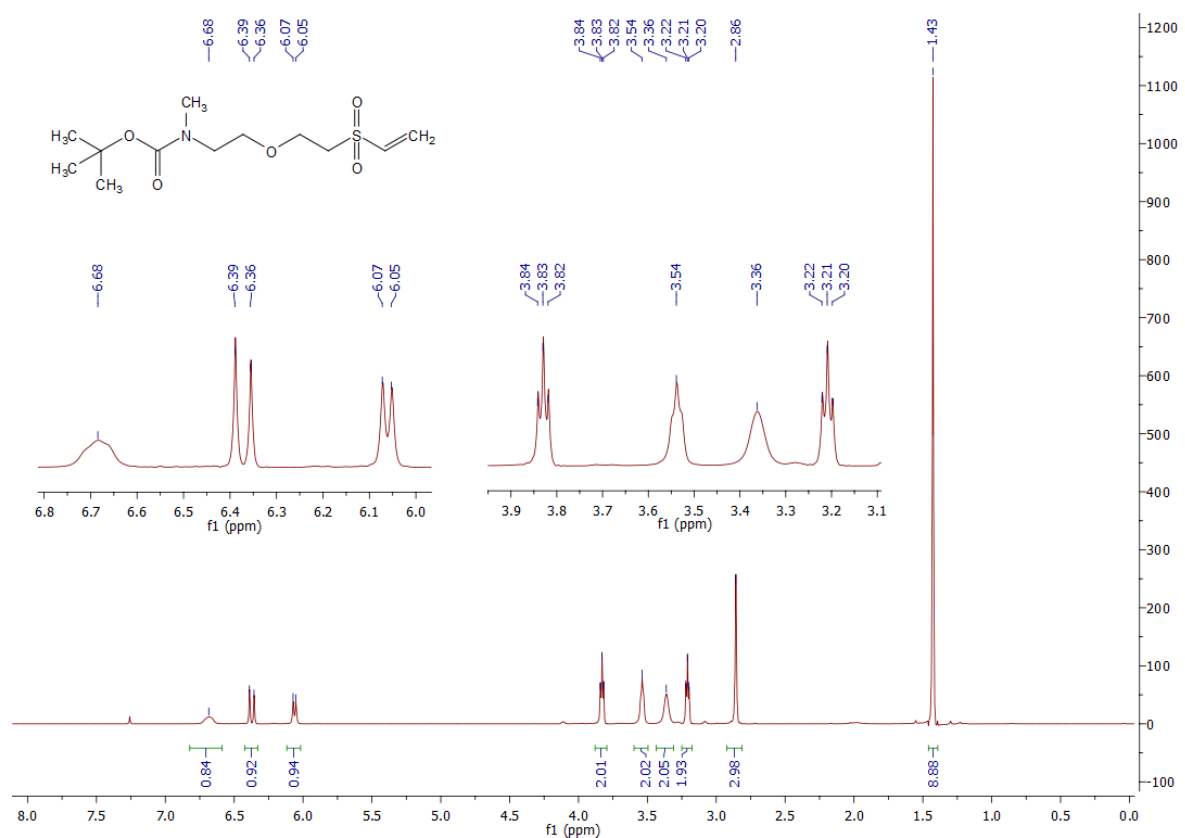


Figure S6. ¹H and ¹³C NMR spectra of *tert*-butyl methyl{2-[2-(vinylsulfonyl)ethoxy]ethyl}carbamate (3)

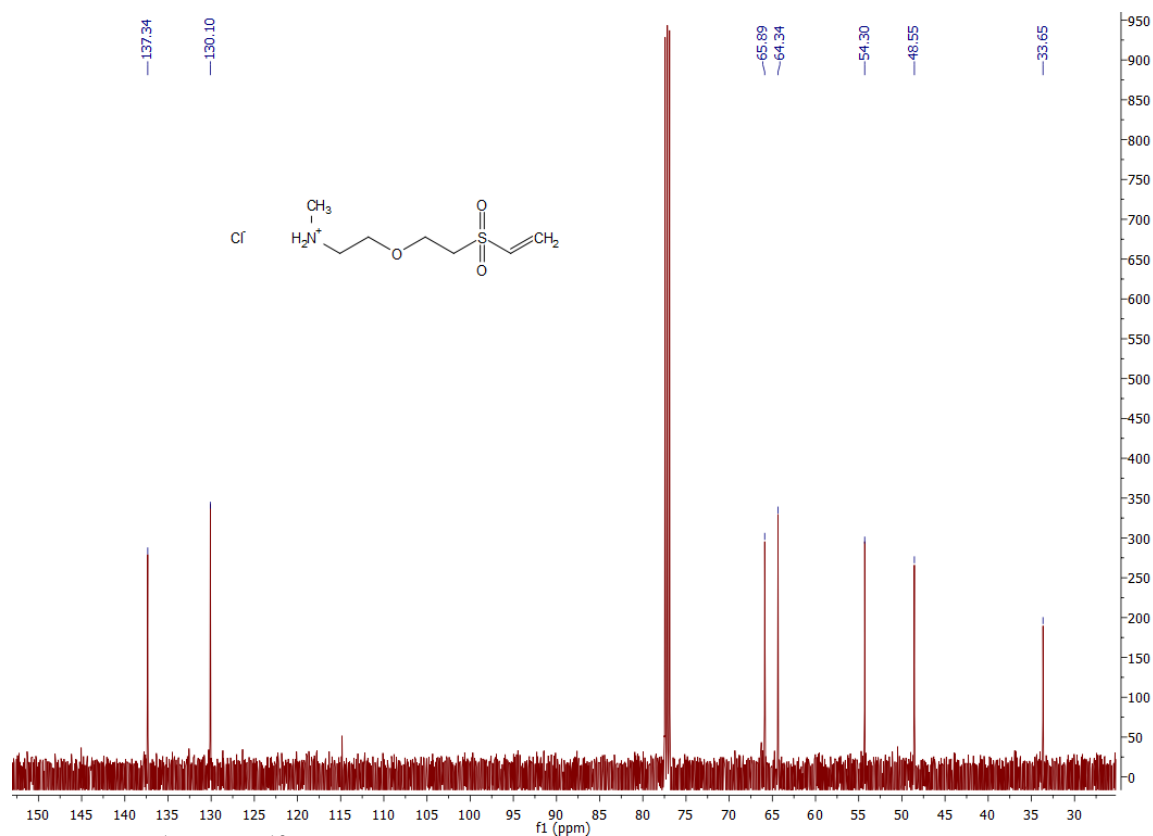
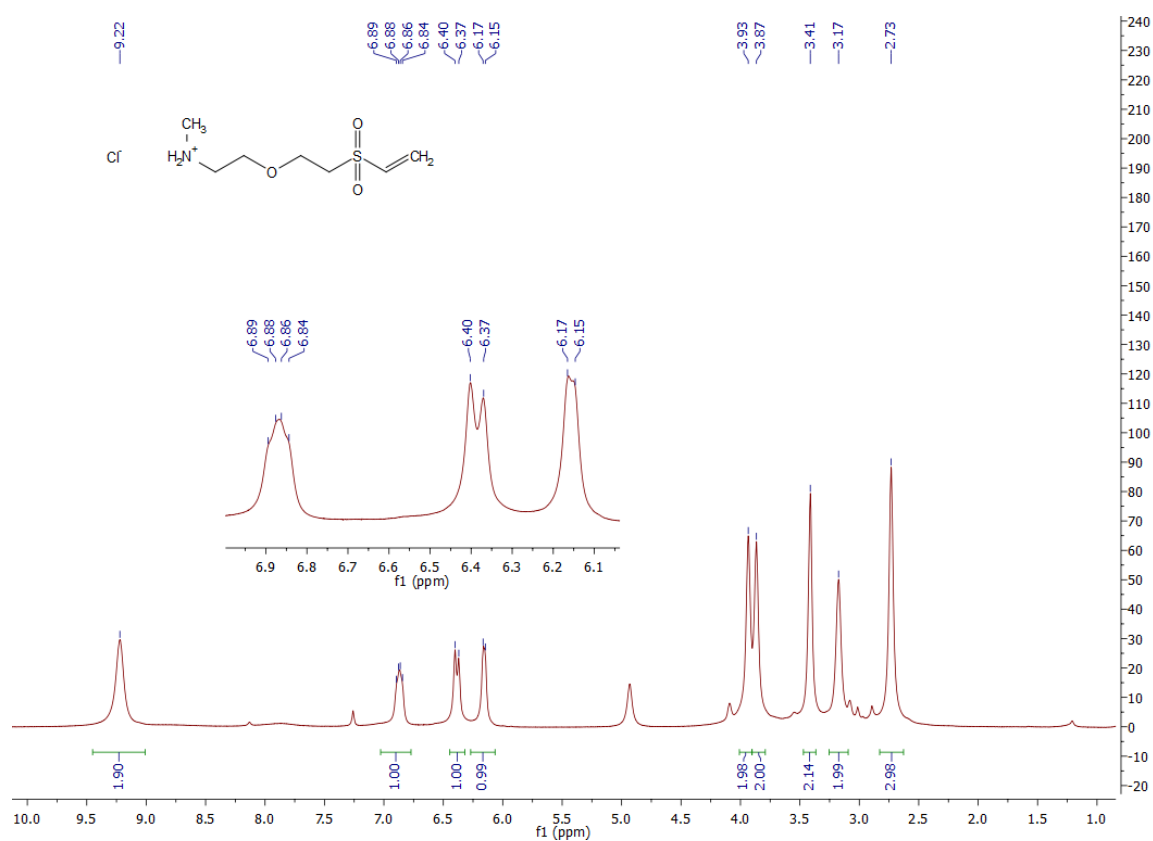


Figure S7. ¹H and ¹³C NMR spectra of *N*-methyl-2-[2-(vinylsulfonyl)ethoxy]ethan-1-amine HCl salt (**4**)

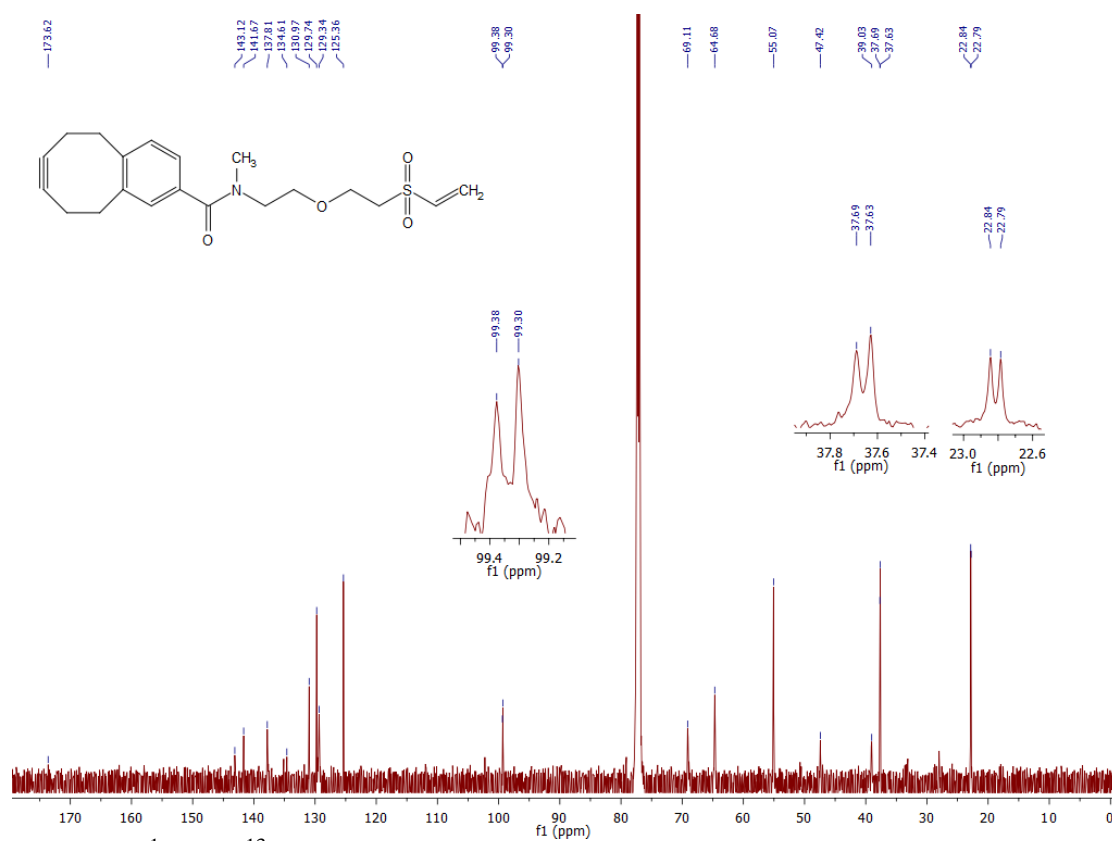
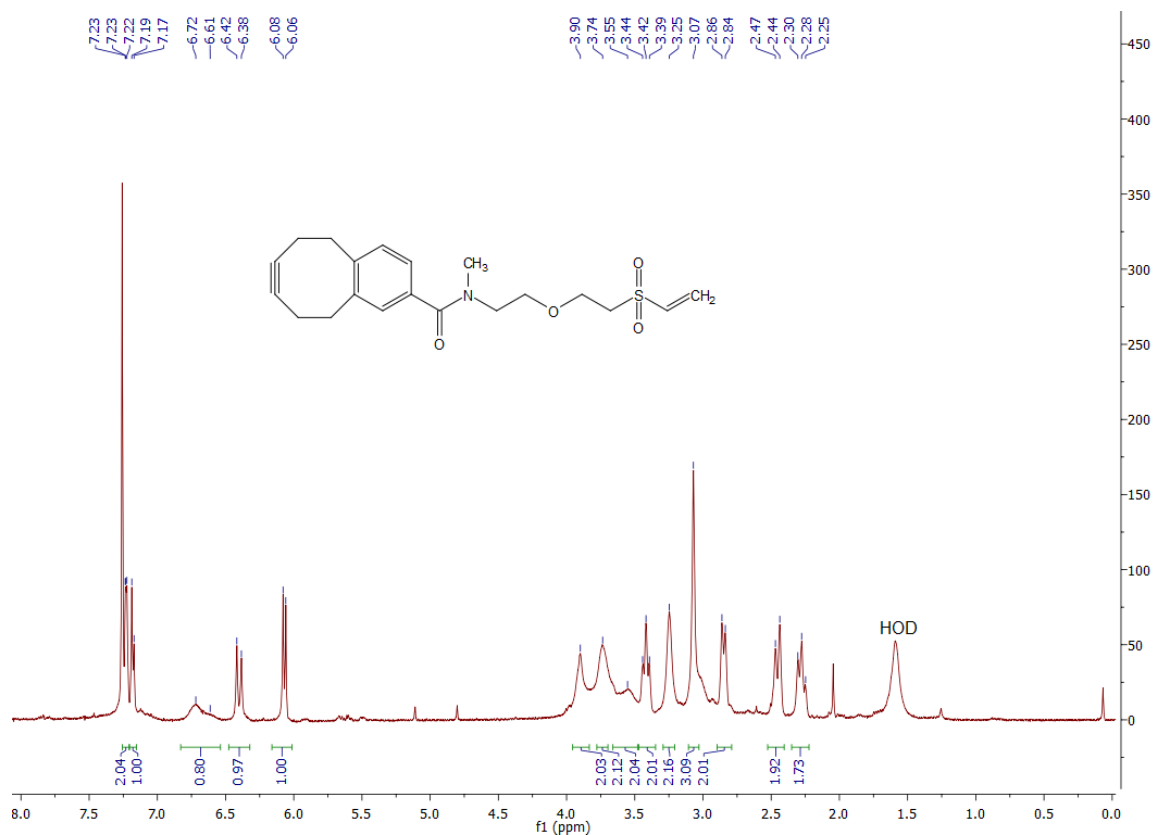


Figure S8. ¹H and ¹³C NMR spectra of LCOMBO

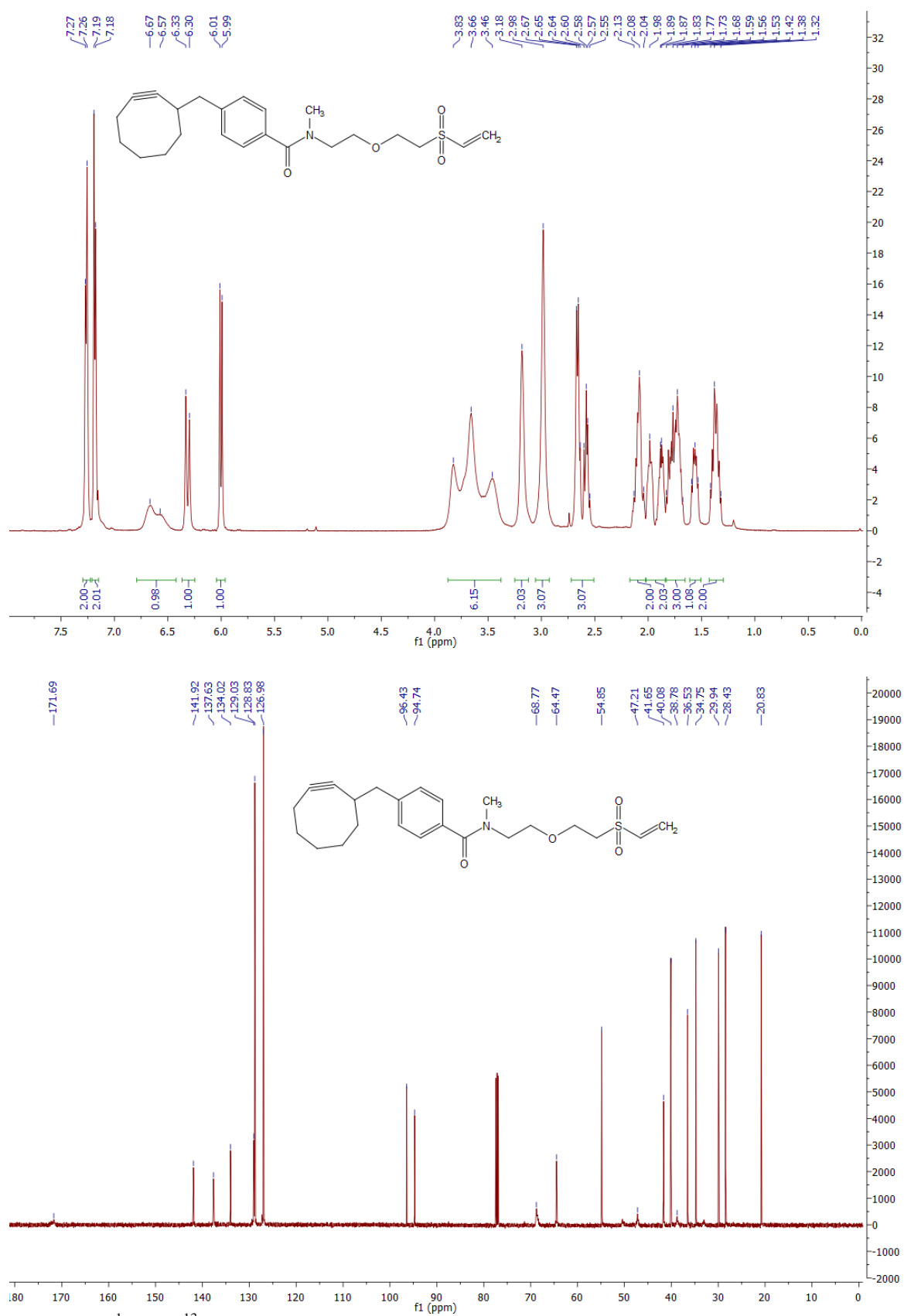


Figure S9. ¹H and ¹³C NMR spectra of L_{cyo}

8. References

- 1 K. Tyagarajan, E. Pretzer and J. E. Wiktorowicz, *Electrophoresis*, 2003, **24**, 2348.
- 2 F. M. Veronese, A. Mero, F. Caboi, M. Sergi, C. Marongiu and G. Pasut, *Bioconjug. Chem.*, 2007, **18**, 1824.
- 3 Y. Kim, S. O. Ho, N. R. Gassman, Y. Korlann, E. V. Landorf, F. R. Collart and S. Weiss, *Bioconjug. Chem.*, 2008, **19**, 786.
- 4 M. Stanley, C. Han, A. Knebel, P. Murphy, N. Shpiro and S. Virdee, *ACS Chem. Biol.*, 2015, **10**, 1542.
- 5 Y. Shiraishi, T. Muramoto, K. Nagatomo, D. Shinmi, E. Honma, K. Masuda and M. Yamasaki, *Bioconjug. Chem.*, 2015, **26**, 1032.
- 6 Y. Chen, C. M. Clouthier, K. Tsao, M. Strmiskova, H. Lachance and J. W. Keillor, *Angew. Chem. Int. Ed. Engl.*, 2014, **53**, 13785.
- 7 S. J. Sirk, T. Olafsen, B. Barat, K. B. Bauer and A. M. Wu, *Bioconjug. Chem.*, 2008, **19**, 2527.
- 8 L. I. Leichert and U. Jakob, *PLoS Biol.*, 2004, **2**, e333.
- 9 K. K. Kannan, M. Ramanadham and T. A. Jones, *Ann. N. Y. Acad. Sci.*, 1984, **429**, 49.
- 10 K. Djcinovic, A. Coda, L. Antolini, G. Pelosi, A. Desideri, M. Falconi, G. Rotilio and M. Bolognesi, *J. Mol. Biol.*, 1992, **226**, 227.
- 11 I. Petitpas, A. A. Bhattacharya, S. Twine, M. East and S. Curry, *J. Biol. Chem.*, 2001, **276**, 22804.
- 12 K. Nishi, T. Ono, T. Nakamura, N. Fukunaga, M. Izumi, H. Watanabe, A. Suenaga, T. Maruyama, Y. Yamagata, S. Curry and M. Otagiri, *J. Biol. Chem.*, 2011, **286**, 14427.
- 13 T. Kinoshita, M. Warizaya, M. Ohori, K. Sato, M. Neya and T. Fujii, *Bioorg. Med. Chem. Lett.*, 2006, **16**, 55.
- 14 S. Sugio, A. Kashima, S. Mochizuki, M. Noda and K. Kobayashi, *Protein Eng.*, 1999, **12**, 439.
- 15 M. E. Smith, M. B. Caspersen, E. Robinson, M. Morais, A. Maruani, J. P. Nunes, K. Nicholls, M. J. Saxton, S. Caddick, J. R. Baker and V. Chudasama, *Org. Biomol. Chem.*, 2015, **13**, 7946.
- 16 A.-L. Marie, C. Przybylski, F. Gonnet, R. Daniel, R. Urbain, G. Chevreux, S. Jorieux and M. Taverna, *Anal. Chim. Acta*, 2013, **800**, 103.
- 17 L. Turell, R. Radi and B. Alvarez, *Free Radic. Biol. Med.*, 2013, **65**, 244.

- 18 G. B. Cserép, Z. Baranyai, D. Komáromy, K. Horváti, S. Bősze and P. Kele, *Tetrahedron*, 2014, **70**, 5961.
- 19 I. Fitos, Z. Tegyei, M. Simonyi, I. Sjöholm, T. Larsson and C. Lagercrantz, *Biochem. Pharmacol.*, 1986, **35**, 263.
- 20 A. Varshney, P. Sen, E. Ahmad, M. Rehan, N. Subbarao and R. H. Khan, *Chirality*, 2010, **22**, 77.
- 21 K. D. Volkova, V. B. Kovalska, M. Y. Losytskyy, A. Bento, L. V. Reis, P. F. Santos, P. Almeida and S. M. Yarmoluk, *Journal of Fluorescence*, 2008, **18**, 877.
- 22 V. S. Jisha, K. T. Arun, M. Hariharan and D. Ramaiah, *The Journal of Physical Chemistry B*, 2010, **114**, 5912.
- 23 A. I. Ivanov, V. B. Gavrilov, D. A. Furmanchuk, O. V. Aleinikova, S. V. Konev and G. V. Kaler, *Clin. Exp. Med.*, 2002, **2**, 147.
- 24 I. Vayá, V. Lhiaubet-Vallet, M. C. Jiménez and M. A. Miranda, *Chem. Soc. Rev.*, 2014, **43**, 4102.
- 25 G. L. Ellman, *Arch. of Biochem. Biophys.*, 1959, **82**, 70.
- 26 F. Zsila, I. Fitos, G. Bencze, G. Kéri and L. Örfi, *Curr. Med. Chem.*, 2009, **16**, 1964.
- 27 H. Sun and P. He, *Chromatographia*, 2008, **68**, 969.
- 28 R. B. Mujumdar, L. A. Ernst, S. R. Mujumdar, C. J. Lewis and A. S. Waggoner, *Bioconjugate Chem.*, 1993, **4**, 105.
- 29 <https://tools.thermofisher.com/content/sfs/brochures/TR0031-Calc-FP-ratios.pdf>.